

Electronic Supplementary Information

Fabrication of a 3D self-supporting Ni-P/Ni₂P/CC composite and their robust hydrogen evolution reaction property in alkaline solution

Fan Yang^a, Shuqin Yang^a, Qianqian Niu^a, Siyue Huo^a, Zimo Song^a, Laizhou Song*^a

^a College of Environmental and Chemical Engineering, Yanshan University, Qinhuangdao 066004, China

* Corresponding author. E-mail address: songlz@ysu.edu.cn. Tel.: +86-335-8387741.
Fax: +86-335-8061569

Supplementary Methods

Calculation of the number of active sites and turnover frequency (TOF)

The number of active sites (n) was determined by CV with a potential window from -0.2 to 0.6 V vs. RHE in 1.0 M PBS (pH = 7) at a scan rate of 50 mV s⁻¹. Assuming a one-electron process for both reduction and oxidation, the upper limit of n could be calculated¹ according to the equation (S1):

$$n = \frac{Q}{2F} \quad (S1)$$

Where Q is the voltammetric charge obtained by integrating the CV curves, F is the Faradic constant (96485 C mol^{-1}).

Then, the turnover frequency (TOF, s^{-1}) was defined² via the following equation (S2):

$$\text{TOF} = \frac{j \times A}{2nF} \quad (S2)$$

Where j is the current density (A cm^{-2}) at a specific overpotential, A is the area of the electrode (cm^2), and n is the number of active sites (mol).

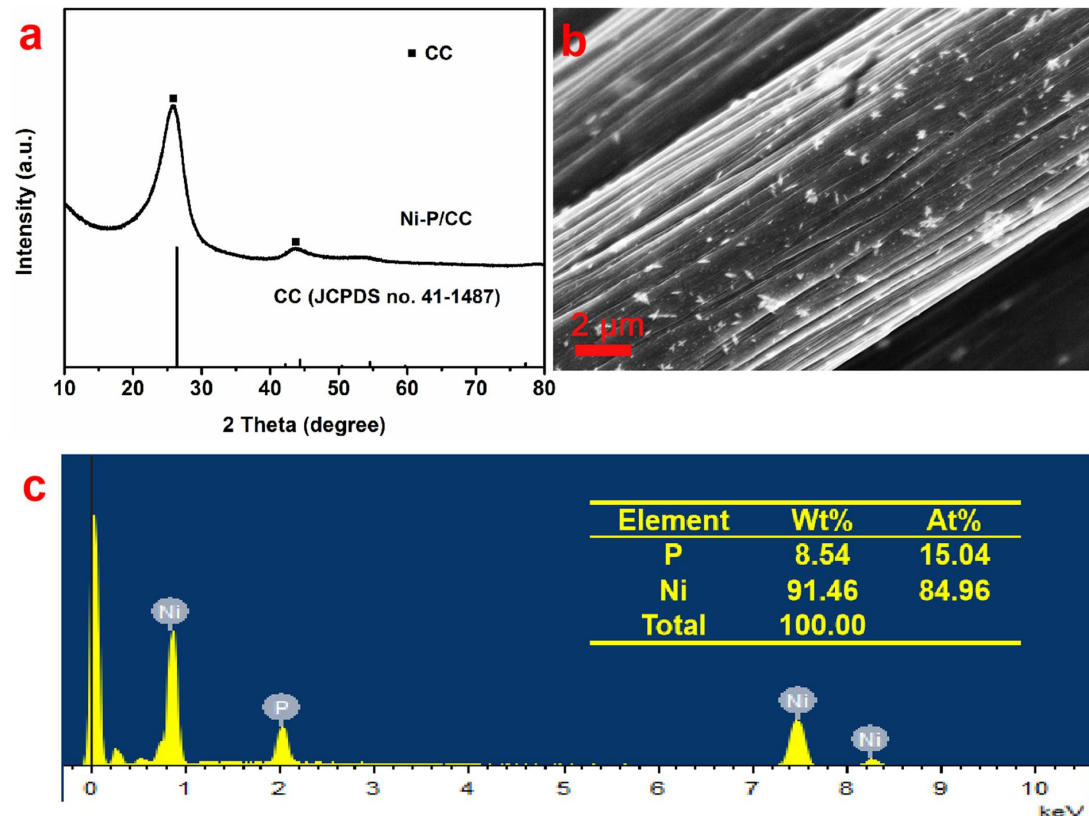


Fig. S1 (a) XRD pattern of Ni-P/CC, (b) SEM image of Ni-P/CC and (c) EDS spectrum of Ni-P/CC with the deposition time of 120 s at the current density of 1 mA cm^{-2} .

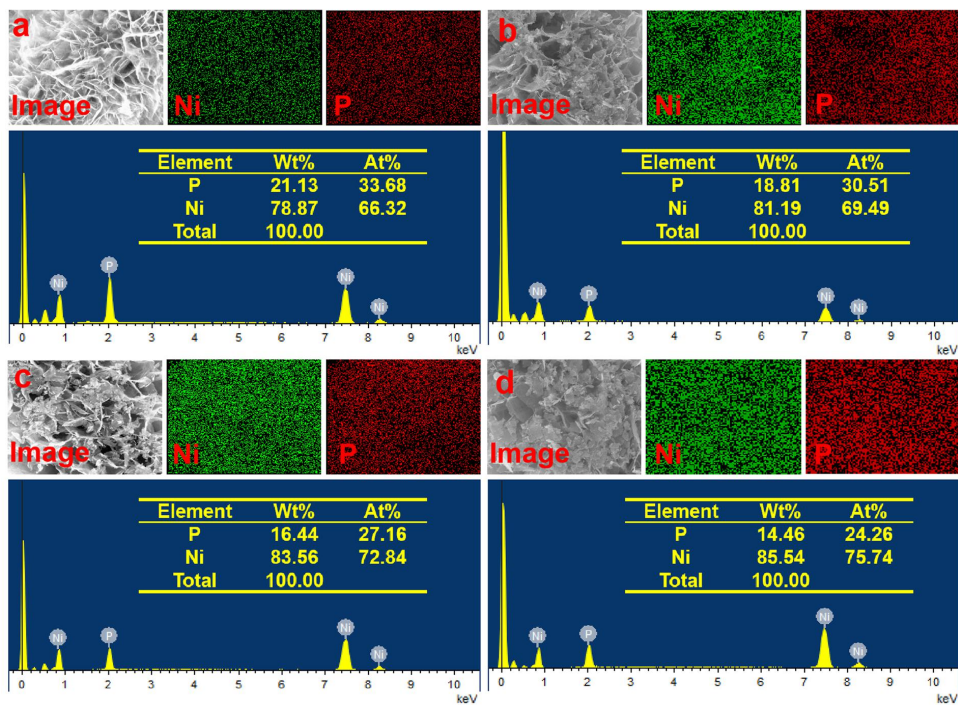


Fig. S2 EDS spectrum of (a) Ni₂P/CC, (b) Ni-P/Ni₂P/CC-1, (c) Ni-P/Ni₂P/CC-2 and (d) Ni-P/Ni₂P/CC-3.

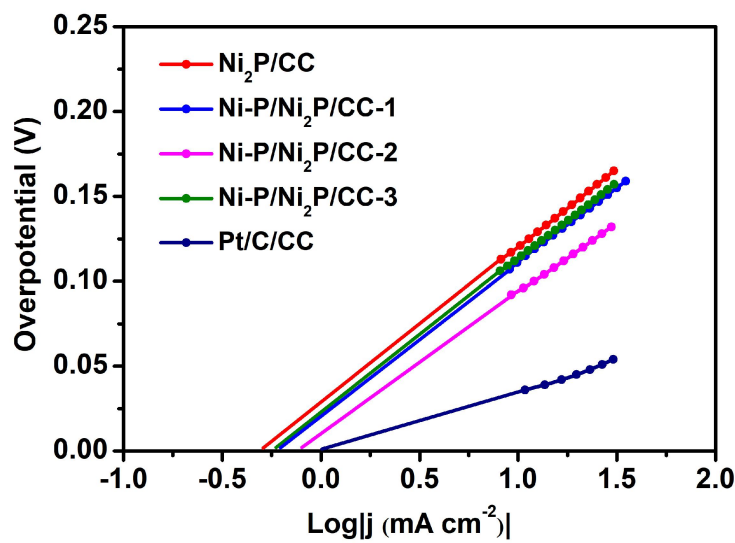


Fig. S3 Calculated exchange current density for Ni₂P/CC, Ni-P/Ni₂P/CC-1, Ni-P/Ni₂P/CC-2, Ni-P/Ni₂P/CC-3, and Pt/C/CC in 1.0 M KOH solution by applying extrapolation of Tafel plot data.

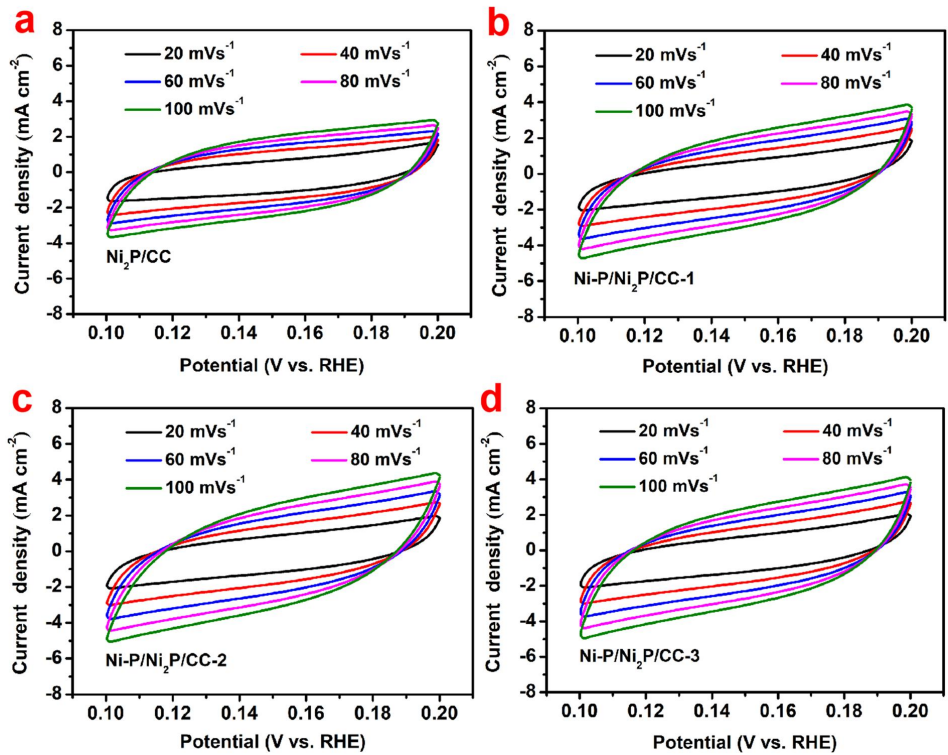


Fig. S4 CV curves of (a) Ni₂P/CC, (b) Ni-P/Ni₂P/CC-1, (c) Ni-P/Ni₂P/CC-2 and (d) Ni-P/Ni₂P/CC-3 in 1.0 M KOH solution at different scan rates.

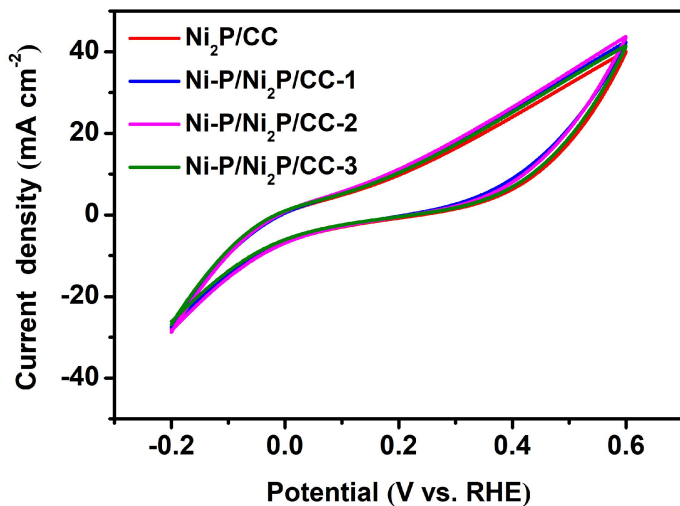


Fig. S5 CV curves of Ni₂P/CC, Ni-P/Ni₂P/CC-1, Ni-P/Ni₂P/CC-2 and Ni-P/Ni₂P/CC-3 in 1 M PBS ($\text{pH} = 7$) with a scan rate of 50 mV s⁻¹.

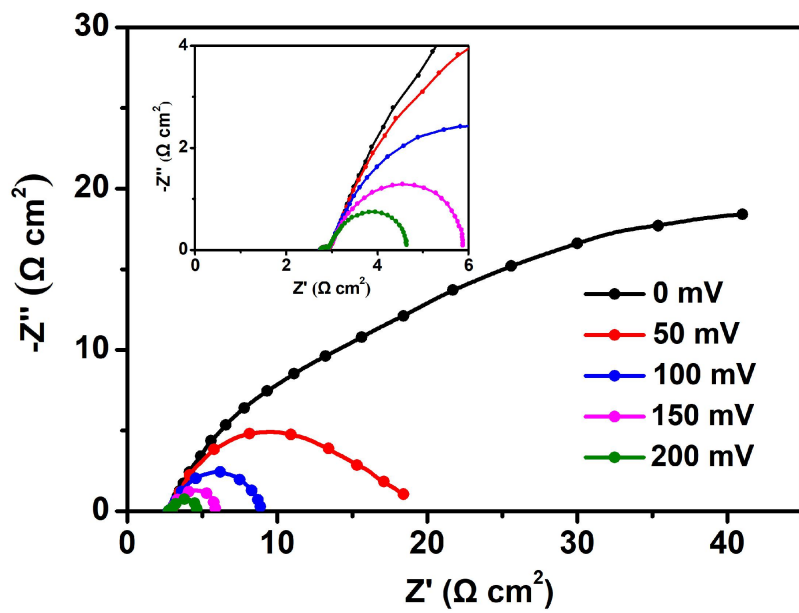


Fig. S6 Nyquist plots of Ni-P/Ni₂P/CC-2 composite at different overpotential values.

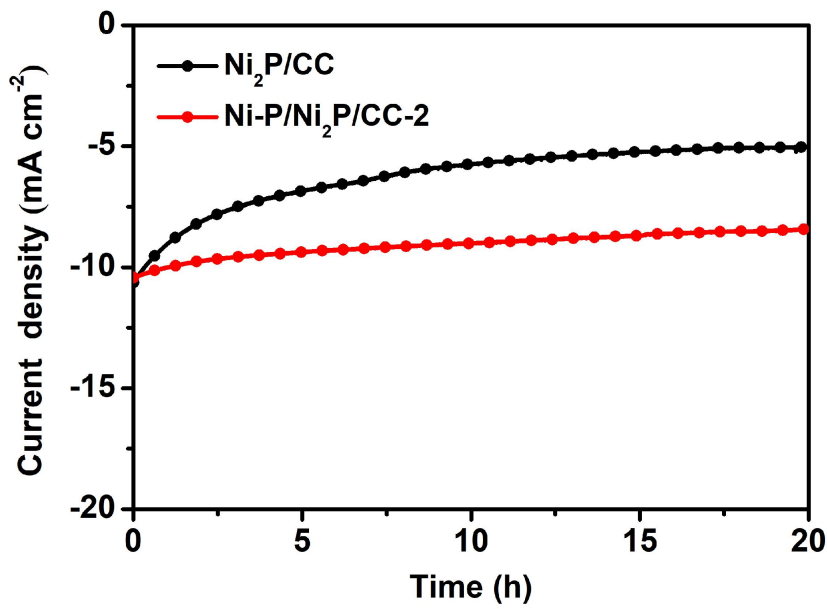


Fig. S7 Time-dependent current density curve of Ni₂P/CC and Ni-P/Ni₂P/CC-2 at a constant overpotential for 20 h in 1.0 M KOH solution.

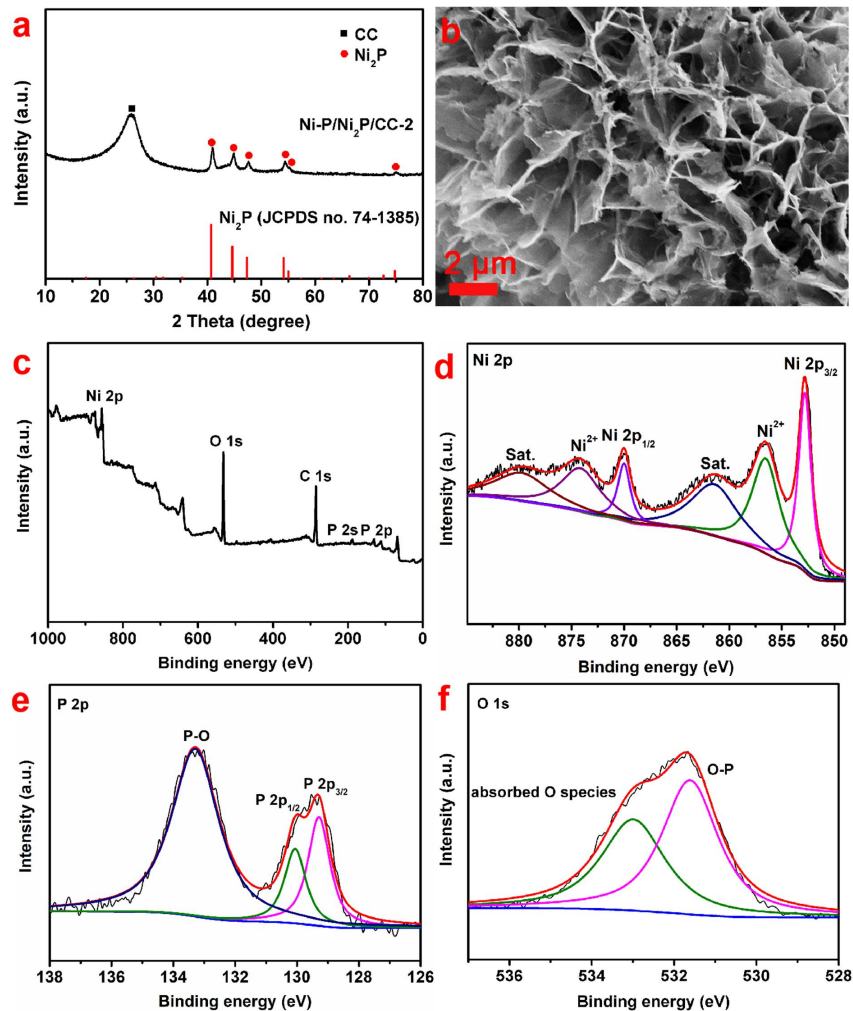


Fig. S8 (a) XRD pattern, (b) SEM image and (c-f) XPS spectra of Ni-P/Ni₂P/CC-2 after long-term stability test in 1.0 M KOH solution.

Table S1 ICP-OES data for Ni-P/CC, Ni₂P/CC, Ni-P/Ni₂P/CC-1, Ni-P/Ni₂P/CC-2 and Ni-P/Ni₂P/CC-3 samples.

Catalyst	Ni (mg cm ⁻²)	P (mg cm ⁻²)	Ni/P atomic ratio
Ni-P/CC	0.033	0.003	5.80
Ni ₂ P/CC	3.073	0.794	2.04
Ni-P/Ni ₂ P/CC-1	3.178	0.706	2.37
Ni-P/Ni ₂ P/CC-2	3.289	0.614	2.82
Ni-P/Ni ₂ P/CC-3	3.367	0.550	3.23

Table S2 Analyzed parameters of the EIS data for Ni₂P/CC, Ni-P/Ni₂P/CC-1, Ni-P/Ni₂P/CC-2 and Ni-P/Ni₂P/CC-3 samples.

Catalyst	R_s ($\Omega \text{ cm}^2$)	Y_1 ($\text{F cm}^{-2} \text{s}^{(n-1)}$)	n_1	R_1 ($\Omega \text{ cm}^2$)	Y_2 ($\text{F cm}^{-2} \text{s}^{(n-1)}$)	n_2	R_{ct} ($\Omega \text{ cm}^2$)
Ni ₂ P/CC	2.44	5.08×10^{-4}	0.742	0.95	1.22×10^{-2}	0.954	4.11
Ni-P/Ni ₂ P/CC-1	2.48	9.63×10^{-2}	0.375	0.41	1.54×10^{-2}	0.952	3.31
Ni-P/Ni ₂ P/CC-2	2.76	3.80×10^{-2}	0.521	0.34	2.03×10^{-2}	0.948	2.81
Ni-P/Ni ₂ P/CC-3	2.65	8.81×10^{-2}	0.511	0.52	1.26×10^{-2}	0.994	3.46

Table S3 Comparison of the HER performances in 1.0 M KOH solution among several reported Ni-based catalysts (GCE is glassy carbon electrode).

Catalyst	Substrates	η_{10} (mV)	Tafel slope (mV dec ⁻¹)	Ref.
Ni-P/Ni ₂ P/CC-2	Carbon cloth	95	80.4	This work
Mn-NiP ₂ NSs/CC	Carbon cloth	97	61	3
Ni ₂ P-Ni ₅ P ₄	Carbon cloth	102	83	4
CP@Ni-P	Carbon paper	117	85.4	5
O ₃ -V10-Ni ₂ P	GCE	108	72.3	6
Ni ₂ P/FeP@NG	GCE	250	91	7
Ni ₂ P/MoS ₂ /N:RGO	GCE	149	60.2	8
Al-Ni ₂ P/TM	Ti mesh	129	98	9
Ni ₂ P/Ni/NF	Ni foam	98	72	10
Cu ₃ P-Ni ₂ P/NF	Ni foam	103	80	11
P-Ni ₂ P/NF	Ni foam	134	92	12

References

- 1 P. Jiang, Q. Liu and X. P. Sun, *Nanoscale*, 2014, 6, 13440–13445.
- 2 W. Gao, M. Yan, H. Y. Cheung, Z. M. Xia, X. M. Zhou, Y. B. Qin, C. Y. Wong,

- J. C. Ho, C. R. Chang and Y. Q. Qu, *Nano Energy*, 2017, 38, 290–296.
- 3 X. D. Wang, H. P. Zhou, D. K. Zhang, M. Y. Pi, J. J. Feng and S. J. Chen, *J. Power Sources*, 2018, 387, 1–8.
- 4 Y. T. Yan, J. H. Lin, K. Bao, T. X. Xu, J. L. Qi, J. Cao, Z. X. Zhong, W. D. Fei and J. C. Feng, *J. Colloid Interface Sci.*, 2019, 552, 332–336.
- 5 X. G. Wang, W. Li, D. H. Xiong, D. Y. Petrovykh and L. F. Liu, *Adv. Funct. Mater.*, 2016, 26, 4067–4077.
- 6 K. N. Dinh, X. L. Sun, Z. F. Dai, Y. Zheng, P. L. Zheng, J. Yang, J. W. Xu, Z. G. Wang and Q. Y. Yan, *Nano Energy*, 2018, 54, 82–90.
- 7 H. Q. Wang, X. Q. Wang, B. J. Zheng, D. X. Yang, W. L. Zhang and Y. F. Chen, *Electrochim. Acta*, 2019, 318, 449–459.
- 8 M. Kim, M. A. R. Anjum, M. Lee, B. J. Lee and J. S. Lee, *Adv. Funct. Mater.*, 2019, 29, 1809151.
- 9 H. T. Du, L. Xia, S. Y. Zhu, F. Qu and F. L. Qu, *Chem. Commun.*, 2018, 54, 2894–2897.
- 10 B. You, N. Jiang, M. L. Sheng, M. W. Bhushan and Y. J. Sun, *ACS Catal.*, 2016, 6, 714–721.
- 11 X. Jin, J. Li, Y. T. Cui, X. Y. Liu, X. L. Zhang, J. L. Yao and B. D. Liu, *Inorg. Chem.*, 2019, 58, 11630–11635.
- 12 X. Jin, J. Li, Y. T. Cui, X. Y. Liu, K. Wang, Y. Zhou, W. J. Yang, X. L. Zhang, C. Zhang, X. Jiang and B. D. Liu, *Int. J. Hydrogen Energy*, 2019, 44, 5739–5747.